MICRORNA-541-5P REGULATES TYPE II ALVEOLAR EPITHELIAL CELL PROLIFERATION AND ACTIVITY BY MODULATING THE HMGB1 EXPRESSION

Jie Shen, Jun Yan, Qiuyun Wang, Lei Zhuang, and Yan Luo

Department of Anesthesiology, Ruijin Hospital, Shanghai Jiaotong University School of Medicine, Shanghai, China

ABSTRACT—Acute lung injury (ALI) is characterized by excessive production of inflammatory factors and alveolar epithelial damage, type II alveolar epithelial (ATII) cells participate in the repairment of the damaged lung tissue in ALI. Recently, microRNAs (miRNAs) have been found to play crucial roles in the amelioration of various inflammation-induced diseases, including ALI. However, the biological function and the mechanisms of action of miRNAs in the regulation of inflammation, and how ATII cells repair damaged lung tissue in ALI remain unknown. In this study, a model of ALI was established using LPS, and ATII cells were isolated and treated with LPS. Hematoxylin and eosin staining revealed the injury to lung tissues. In this study we found that miR-541-5p expression was significantly decreased in ALI tissue and in the LPS-induced ATII cell model. Additionally, the LPS-induced model showed suppression of ATII cell proliferation and activity. Furthermore, overexpression of miR-541-5p was found to promote cell activity and proliferation in the LPS-induced ATII cell model. Moreover, a luciferase assay illustrated that HMGB1 is a target of miR-541-5p, HMGB1 knockdown blocked the inhibitory effect of miR-541-5p on LPS-induced ATII cells. Ultimately, our study demonstrated that expression of p38, JNK, and ERK in LPS-induced ATII cells increased significantly. These results suggest that miR-541-5p is a key effector in ALI tissue, and that LPS-induced ATII cells act by regulating HMGB1 expression. This effect may be related to excessive activation of the JNK/ERK/p38 signaling pathway.

KEYWORDS—Acute lung injury, alveolar epithelial cells, HMGB1, miR-541-5p, type II

INTRODUCTION

Acute lung injury (ALI) is characterized by uncontrolled pulmonary inflammation. Many studies have suggested that excessive inflammation resulting in alveolar epithelial cell injury is central to the pathogenesis of ALI, and that the diffuse damage to the alveolar epithelial barrier leads to a high mortality (1, 2). Recent epidemiologic studies have reported that ALI remains a major challenge for clinicians and is an important public health problem globally (3). Type II alveolar epithelial (ATII) cells are progenitor cells that can differentiate into type I alveolar epithelial (ATI) cells to promote re-epithelization of impaired alveoli, and the secretion of alveolar surfactant reduces surface tension and prevents collapse of the alveoli (4, 5). Therefore, repair and regeneration of injured ATII cells is critical in the alleviation of lung injury.

MicroRNAs (miRNAs) comprise 18 to 23 nucleotides (NTs) noncoding small RNAs that modulate both the translation and stability of targeted mRNA (6). Aberrant expression of miR-NAs is linked to many pathological conditions, including cancer and cardiovascular disease. A large number of studies have pinpointed the aberrant expression of miRNAs in the onset and development of inflammatory lung diseases, including ALI (7). The essential role of miRNAs in ALI indicates that miRNAs might be a useful therapeutic target for the treatment of ALI. Previous studies have demonstrated that miR-541-5p is a key effector in lung pulmonary fibrosis. However, the precise mechanism of the effect of miR-541-5p on LPS-induced ATII cell viability and proliferation *in vitro* remains elusive.

Accumulating evidence suggests that inflammation plays a pivotal role in the pathogenesis of ALI, and that suppression of inflammation results in a reduction of the severity of ALI damage (8). High-mobility group box-1 (HMGB1) is a highly conserved nuclear protein that has been widely investigated as a putative danger signal for various inflammatory diseases (9, 10), it has also been proposed as a therapeutic agent for ALI (11, 12). Previous studies have shown that HMGB1 was able to influence the normal function of vascular endothelial cells in ALI (13), suggest that the progression of alveolar epithelial cell injury in ALI may be mediated by HMGB1 signaling, implying that it is a potential therapeutic target for these conditions.

Of note above, whether miR-541-5p affected the progression of ALI via modulating the cellular function of ATII cell remains unknown. Thus, the aim of this study was to dissect the role and underlying mechanism of miR-541-5p in the ALI and the pathophysiology in ATII cell.

MATERIALS AND METHODS

Animal preparation

C57BL/6 mice (4 6 weeks old; 18 22 g of weight) were purchased from Shanghaijiaotong University with the animal license of SCXK (hu) 2017 0011. All animal experiments were performed in accordance with the standards established by the Institutional Animal Care and Use Committee at Shanghai Jiaotong University Medical School. These mice were raised in a specific pathogen-free animal laboratory, and the Physical Laboratory was the responsible unit. Briefly, male mice that were randomized into three groups (Sham, LPS injection 6 h, LPS injection 12 h) of six per group were anesthetized and used as a model of direct lung injury with LPS. The abdominal skin of the rats was disinfected with iodophor, then wiped with cotton, and the LPS solution was injected intraperitoneally at a dosage of 10 mg/kg body weight. Control mice were treated with isovolumetric physiological saline.

Isolation of ATII cells

The ATII cells were isolated at 90% to 95% purity from 6-week-old C57BL/6 mice following the procedure described by Corti et al. (14). Briefly, the mice were killed, the pulmonary artery was cannulated, and the lungs were perfused with normal saline *in situ* to deplete blood. Then, the fresh lungs were excised carefully, transferred on ice, dissected free, minced with sharp scissors, and placed in 5 mL dispase to digest them at room temperature for 60 min with gentle rocking. Pancreatic DNase (0.01% in DMEM) was added for the final 5 min of the incubation. The lung suspension was filtered through strainers of 100, 200, and 400 sterile meshes. After centrifugation and removal of the supernatant, the cells were gently suspended in DMEM (low glucose) without fetal bovine serum. We coated 100 mm bacteriologic plastic dishes with 5 mL of 0.05% pig IgG solution. The IgG solution was adhered for 3 h at 37°C and was then removed from the dishes. The dishes were washed twice with 10 mL of phosphate-buffered saline (PBS) and once with 10 mL DMEM. Nonadherent cells were collected, pelleted by centrifugation, resuspended in normal saline, and counted using a hemocytometer. Cells were cultured in air containing 5% CO_2 in a humidified atmosphere at 37°C.

Hematoxylin and eosin (H&E) staining

Lung tissues collected from mice at 6 h and 12 h after LPS intraperitoneal injection were inflated with 10% buffered formalin for 24 h, fixed with 10% buffered formalin, embedded in paraffin, and tissue sections (5 μm) were cut and stained with hematoxylin and eosin (H&E) for 5 min. The pathological changes in the lung tissues were then examined under a light microscope.

RNA interference and cell transfection

miR-541-5p and HMGB1-specific RNAi oligonucleotides (siRNA) were designed and synthesized by GenePharma (Shanghai, China). miR-541-5p mimics and inhibitors were purchased from RiboBio (Guangzhou, China). The sequences of siRNAs were as follows: shHMGB1-1: 5′-CACCCGGAT-GCTTCTGTCAACTTCT-3′; shHMGB1-2: 5′-GGCAAAGGCTGACAAGG-CTCGTTAT-3′; shHMGB1-3: 5′-CCTTCGGCCTTCTTCTTGTTCT GTT-3′; mmu-miR-541 mimics: 5′-AAGGGAUUCUGAUGUUGGUCACACU-3′; mmu-miR-541 inhibitor 5′-AGUGUGACCAACAUCAGAAUCCCUU-3′. The RNA oligonucleotides were transfected into ATII cells using Lipofectamine® 2000 (Invitrogen, Carlsbad, Calif) in Opti-MEM culture medium. ATII cell samples were collected subsequently and analyzed after culturing for 48 h.

Total RNA isolation and quantitative real-time reverse transcription-PCR

The total RNA of ATII cells with the different treatments was extracted using Trizol reagent (Invitrogen) according to the manufacturer's protocol. The RNA concentrations were detected with a NanoDrop ND-1000 spectrophotometer (Thermo Fisher Scientific). Reverse transcription (RT) was performed using the EasyScript One-Step gDNA Removal and cDNA Synthesis SuperMix (Transgen Biotech, Shanghai, China). Real-time RT-PCR amplification was performed with 10 ng of cDNA using the SYBR Green reagent (Thermo Fisher Scientific) on the Prism 7500 SDS system (Applied Biosystems, Foster City, Calif). Relative mRNA and microRNA expression levels were normalized to GAPDH (glyceraldehyde 3-phosphate dehydrogenase) or U6 snoRNA. The primers for the various genes were as follows: miR-541-5p forward: 5′-GTCGTATCCAGTGCAGG GTCCGAGG-TATTCGC-3′; reverse: 5′-ACTGGATACGACAGTG TG-3′; HMGB1 forward: 5′-ACTTGGCAAAGCAAGGAGTGA-3′; reverse: 5′- GCCAGCGTTCTTGTGA-TAGC-3′; β-actin forward: 5′-CACTGTCGAGTCCGCGT-3′; reverse: 5′- GCAT-CATCTCCCGCG AA-3′.

Western blot analysis

The cells samples with different treatments were extracted using RIPA lysis buffer (Thermo Fisher Scientific). Whole-cell lysates from ATII cells with the different treatments were subjected to SDS-PAGE (sodium dodecyl sulfate-polyacrylamide *gel* electrophoresis) using 12% polyacrylamide gels. Proteins were then transferred to the Pure Nitrocellulose Blotting membrane (Millipore, Billerica, Mass). The membranes were incubated with anti-HMGB1 antibody (Ab79823, Abcam), anti-p-JNK antibody (#9251, CST), anti-JNK antibody (#9252, CST), anti-p-ERK antibody (#4370, CST), anti-ERK antibody (#4695, CST), anti-p-38 antibody (#4511, CST), anti-p-38 antibody (#8690, CST), and anti-β-actin antibody (AY0573, Abways) at 4°C overnight, followed by three washings with PBS (10 min each). After that, the membranes were incubated with horseradish peroxidase-conjugated secondary antibody (1:2,000 dilution; Thermo Fisher Scientific) at room temperature for 1 h and then washed three times with PBS (10 min each). The immunoreactivity was visualized using the Chemiluminescence Detection Kit (Donghuan Biotech, Shanghai, China) and the data were analyzed using Gel-pro Analyzer Software. GAPDH was used as the loading control

Luciferase reporter assay

The starBase web server v2.0 was used to predict the interaction between miR-541-5p and HMGB1. The wild-type reporter construct was obtained by cloning HMGB1 3′ UTR sequences that were amplified by PCR technique into the psiCHECK-2 luciferase reporter plasmid (Promega, Madison, Wis). The putative binding site was mutated as HMGB1-Mut. In brief, HEK293T cells (Cobioer, Najing, China) were cotransfected with the HMGB1-Wt or Mut 3′ UTR reporter plasmids (2 μg), and miR-541-5p mimic (50 nM). Forty-eight hours after transfection, luciferase activities were examined using the Dual-Luciferase Reporter Assay System (Promega).

Cell viability assay

The viability of ATII cells was detected using Cell Counting Kit-8 (CCK-8) [Donghuan Biotech] following the manufacturer's instructions. Briefly, the ATII cells with different treatments were seeded in a 96-well plate. Then, the CCK-8 solution (10% of the medium, 10 μL) was added to each well and incubated for 4 h. The absorbance at 450 nm was then measured using a microplate reader. Data were recorded as the cell number change relative to the control.

Enzyme-linked immunosorbent assay (ELISA)

The content of tumor necrosis factor-α (TNF-α), and interleukin-6 (IL-6) in lung tissue and ATII-cells were measured on the basis of the instructions of the commercial kit's protocol (Meilian Biotech (ml063159, ml002095, China). The absorption was determined at the wavelength of 450 nm.

EdU incorporation assay

The ATII cells were seeded in 24-well tissue culture plates at a density of 1,500 cells per well. Next, 5-ethynyl-2′-deoxyuridine (EdU) [Donghuan Biotech] was added to each well and incubated for 2 h after hypoxia treatment. The cells were then fixed with 4% paraformaldehyde for 30 min at room temperature, followed by incubation with Apollo Staining reaction liquid (RiboBio, Guangzhou, China) to detect the positive cells. Hoechst (Sigma) was used for nuclear staining. Immunofluorescence was detected by fluorescence microscopy (Zeiss, Oberkochen, Germany).

Statistical analysis

All experiments were performed in triplicate. Data were expressed as the mean ± standard error of the mean (SEM), and analyzed using GraphPad Prism 5.01 (GraphPad Software). Differences between three or more groups were analyzed using one-way analysis of variance followed by the Tukey test for *post hoc* tests for variables with a normal distribution or the Kruskal–Wallis test followed by the Dunnett t test for those without a normal distribution. Differences between two groups were analyzed using the two-tailed unpaired Student t test for variables with a normal distribution or the Mann–Whitney test for variables without a normal distribution. A P value < 0.05 indicates a significant difference.

RESULTS

Histology and inflammatory proteins in LPS-induced ALI

H&E staining showed serious hyperemia in the lung tissues and marked inflammatory cell and red blood cell infiltration in the alveolar spaces, but in contrast, there were no obvious
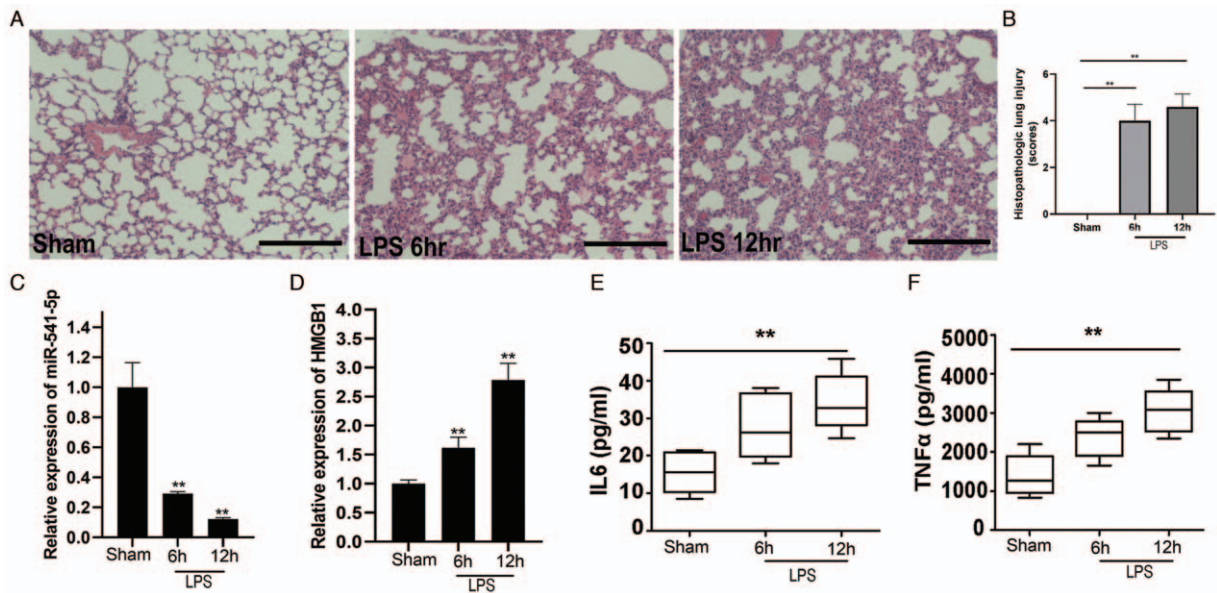
FIG. 1. **miR-541-5p was downregulated in LPS-induced acute lung injury in mice.** A, Histological changes in lung tissues of LPS-induced ALI mice, as evaluated by H&E staining; scare bar, 10 μm. B, Lung inflammation score. C, The miR-541-5p level in lung tissue samples was measured by qRT-PCR (n = 3/group). D, The HMGB1 level in lung tissue samples was measured by qRT-PCR (n = 3/group). E, F, IL-6 and TNF-α levels in lung tissue were measured at 12 h after LPS intervention (n = 3/group). Data are presented as means ± SD of three individual experiments. **$P < 0.01$ vs control group.
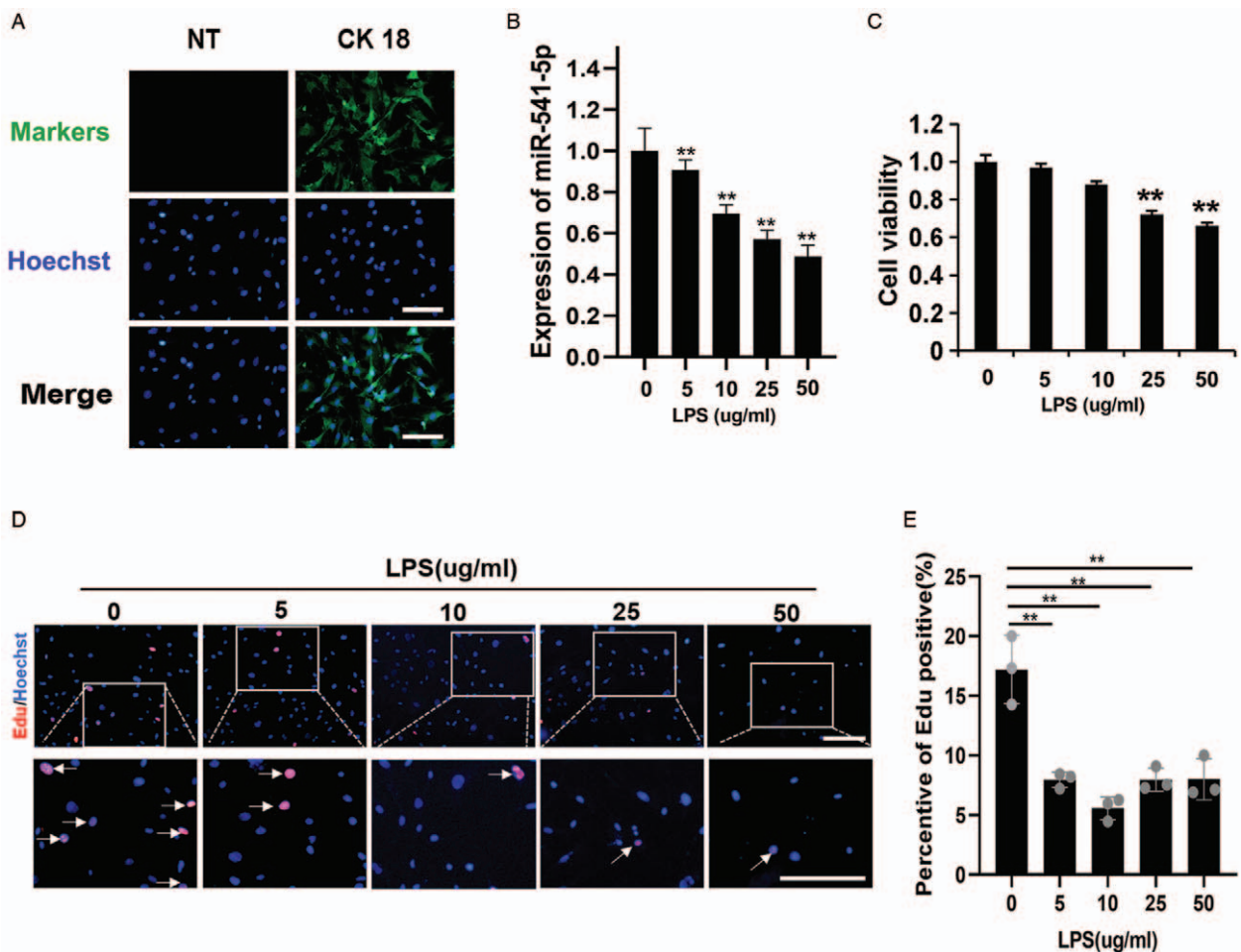

FIG. 2. **miR-541-5p was downregulated in LPS-induced ATII cells.** A, Identification of ATII cells by immunofluorescence staining. B, Expression levels of miR-541-5p were analyzed by real-time quantitative PCR (qRT-PCR). C, CCK8 assay analyses of the cell viability potentials of ATII cells treated with LPS at different concentrations. D, E, EdU assay analyses of the cell proliferation of ATII cells treated with LPS at different concentrations; scare bar, 50 μm. Data are presented as means ± SD of three individual experiments. *$P < 0.05$ and **$P < 0.01$.

pathological changes in the control group (Fig. 1A and B). Levels of tumor necrosis factor (TNF)-α and interleukin (IL)-6 were determined using ELISA (enzyme-linked immunosorbent assay), the results of which indicated that levels of both TNF-α and IL-6 induced by LPS treatment were effectively increased in lung tissues (Fig. 1E and F).

LPS inhibits the activity and proliferation of ATII cells, miR-541-5p was significantly decreased in ALI tissues and LPS-induced ATII cells

To investigate the function of ATII cells in LPS intervention, primary cultured ATII cells were treated with LPS at different concentrations (Fig. 2A) and cell viability and proliferation were then measured. CCK8 and EdU analysis showed a reduction of the activity and proliferation of LPS-induced ATII cells (Fig. 2C–E). We detected the expression of miR-541-5p in LPS-induced ATII cells by qRT-PCR. The results showed that miR-541-5p was markedly decreased in LPS-induced ATII cells (Fig. 2B), consistent with ALI tissues (Fig. 1C). These results indicate that LPS exerts its function by reducing the viability and migration of ATII cells, miR-541-5p might play an important role in ALI and in LPS-induced ATII cells.
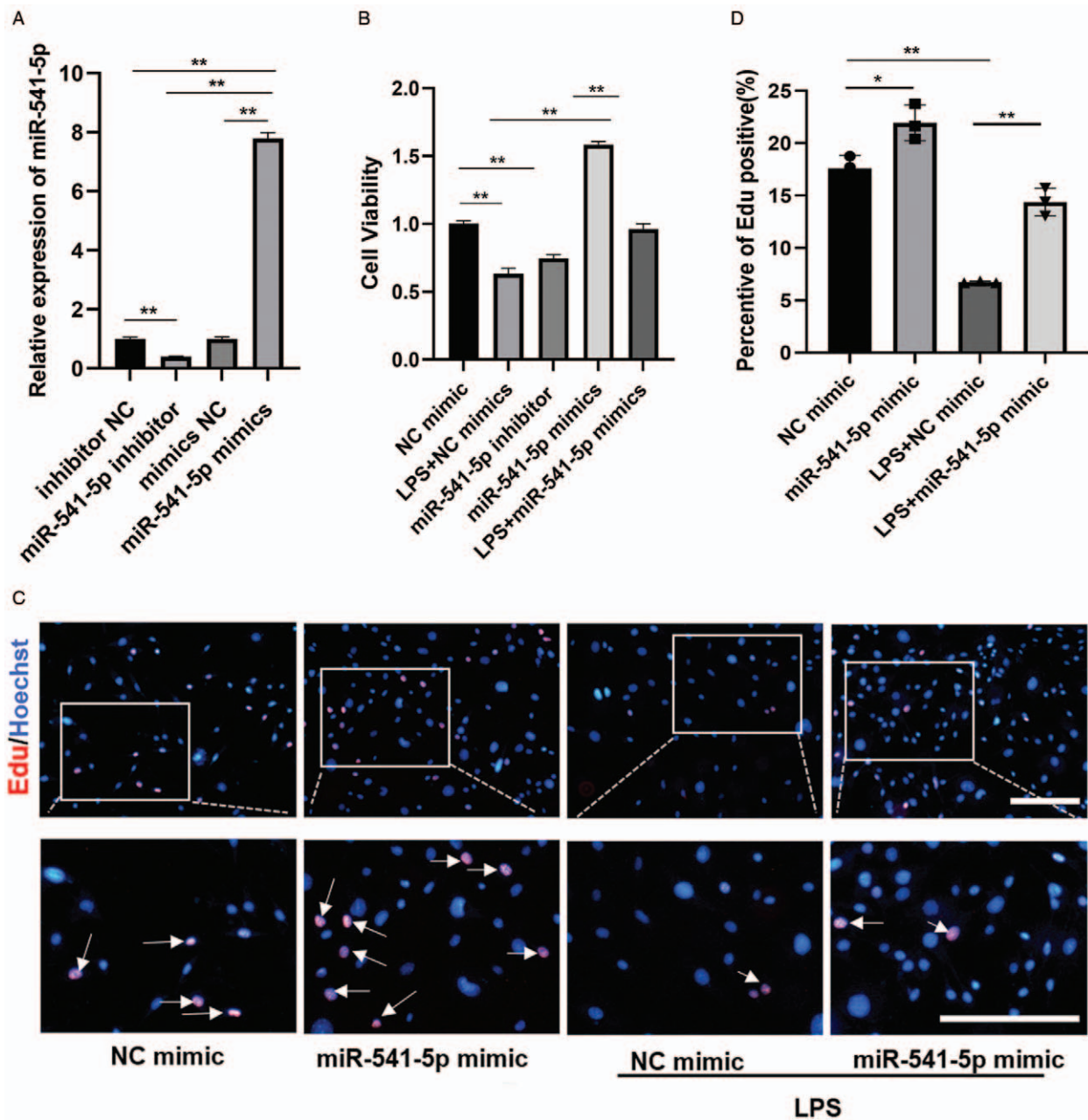

Fig. 3. **Upregulation of miR-541-5p played a crucial role in ATII cells treated with LPS.** A, qRT-PCR analyses of the expression of miR-541-5p in ATII cells treated with inhibitor NC, miR-541-5p inhibitor, NC mimics, and miR-541-5p mimics. B, CCK8 assay analyses of the cell viability potentials of ATII cells treated with NC mimics, miR-541-5p mimics, LPS + NC mimics, miR-541-5p inhibitor, and LPS + miR-541-5p mimics. C, D, EdU assay analyses of the cell proliferation of ATII cells treated with NC mimics, miR-541-5p mimics, LPS + NC mimics, and LPS + miR-541-5p mimics; scare bar, 50 μm. Data are presented as means ± SD of three individual experiments. $^{*}P < 0.05$ and $^{**}P < 0.01$.

MiR-541-5p regulated the activity and proliferation of LPS-induced ATII cells

To further clarify the role of miR-541-5p in LPS-induced ATII cells, we investigated the function of miR-541-5p on ATII cell activity and proliferation. CCK8 and EdU analysis showed decreased activity and proliferation of LPS-induced ATII cells. These results indicate that LPS exerts its function by reducing the viability and proliferation of ATII cells. Additionally,

overexpression of miR-541-5p was found to partly reverse the LPS-induced ATII cell activity and proliferation (Fig. 3B–D).

miR-541-5p regulates the activity and proliferation of ATII cells by HMGB1 in ATII cells

To confirm the regulation of HMGB1 by miR-541-5p, the dual-luciferase reporter assay was used to detect binding
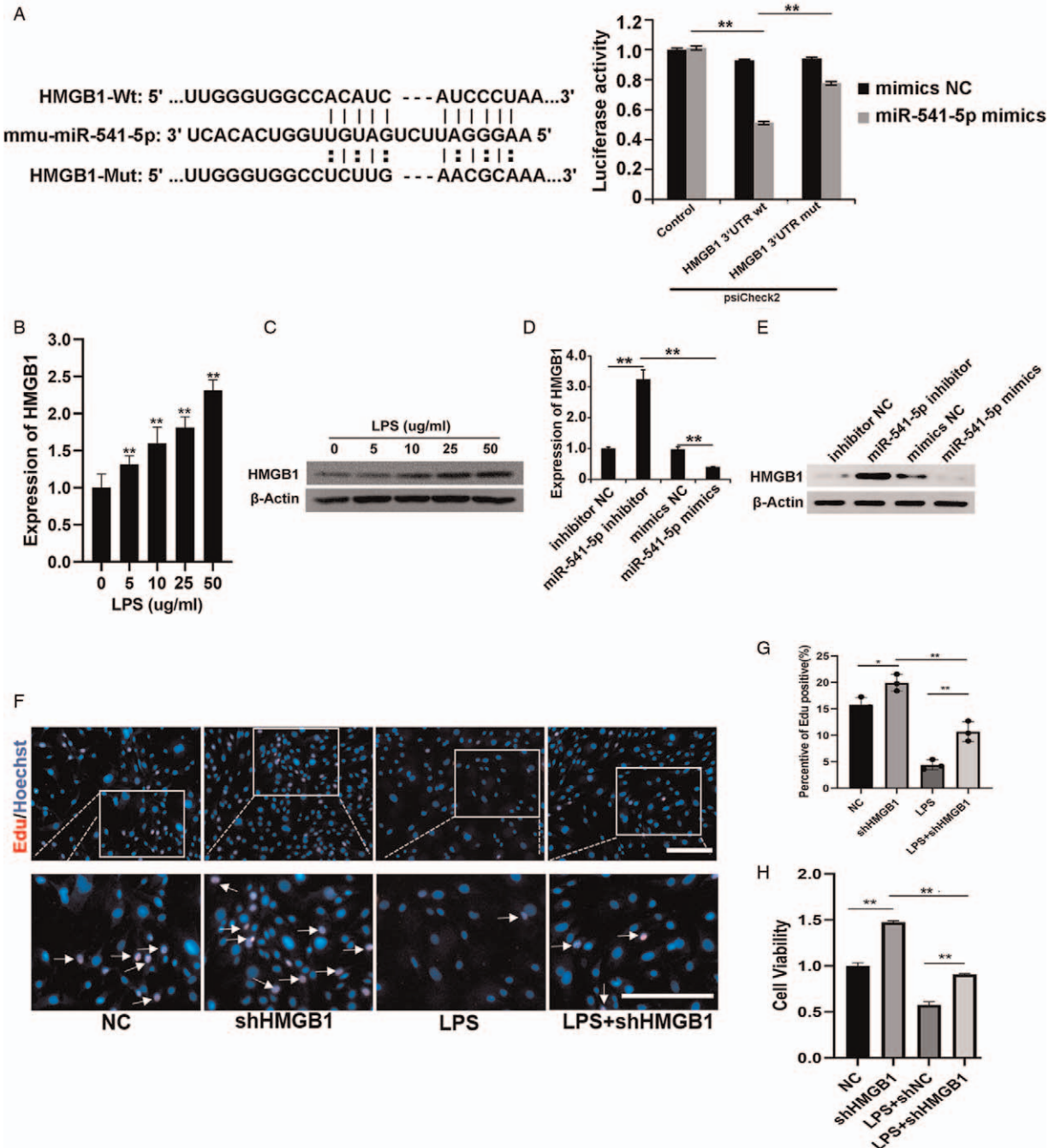

Fig. 4.   **miR-541-5p exerted its role by regulating HMGB1 in ATII cells treated with LPS.** A, Luciferase assay of HEK293 cells cotransfected with firefly luciferase constructs containing the HMGB1 wild-type or mutated 3'-UTRs and miR-541-5p mimics, and NC mimics, as indicated (n = 3). B, C, qPCR and western blot analyses of the expression of HMGB1 in ATII cells treated with LPS at different concentrations. D, E, qPCR and western blot analyses of the expression of HMGB1 in ATII cells treated with NC, shHMGB1, LPS, LPS + shHMGB1. F, G, EdU assay analyses of the cell proliferation of ATII cells treated with NC, shHMGB1, LPS, and LPS + shHMGB1. H, CCK8 assay analyses of the cell viability potentials of ATII cells treated with NC, shHMGB1, LPS, and LPS + shHMGB1. Data are presented as means ± SD of three individual experiments. β-Actin served as a control; scare bar, 50 μm. $^{*}P < 0.05$ and $^{**}P < 0.01$.

between miR-541-5p and HMGB1. The results showed that miR-541-5p mimics the inhibited luciferase activity of the wild-type HMGB1 reporter, but no changes were observed in target identification and validation (Fig. 4A). Furthermore, expression of HMGB1 was increased in LPS-induced ATII cells (Fig. 4B and C), miR-541-5p inhibitor upregulated the expression of HMGB1, whereas overexpression of miR-541-5p decreased the mRNA expression of HMGB1 (Figs. 4D, E, 5A, B). Moreover, CCK8 and EdU analysis showed increased activity and proliferation of LPS-induced ATII cells when HMGB1 was inhibited (Figs. 4F, G, 5C). Result confirms that HMBG1 is regulated by miR-541-5p in ATII cells.

microRNA-541-5p regulates type II alveolar epithelial cell proliferation and activity by modulating the HMGB1/JNK/ERK/p38 pathway

To confirm the regulation of HMGB1/JNK/ERK/p38 pathway by miR-541-5p, p-JNK, p-ERK, and p-p38, which belong to the MAPK family, were detected in LPS-induced ATII cells. Western bolt showed the expression of p-JNK, p-ERK, and p-p38 were increased, while overexpression of miR-541-5p

suppresses expression (Fig. S1, http://links.lww.com/SHK/B361, S2, http://links.lww.com/SHK/B362)

DISCUSSION

ALI is one of the most serious complications of sepsis and it remains an obstinate condition, characterized by serious damage to the alveolar capillary membrane (15, 16). Many studies have shown that ATII cells are the main progenitor cells in restoring the alveolar epithelium after injury (17, 18). Previous studies have demonstrated that promotion of ATII cell proliferation and activation is an effective way to attenuate lung injury (19).

A large number of miRNAs are expressed in the lung and are involved in respiratory diseases, including ALI (20, 21). These miRNAs widely influence the signaling networks, leading to pathological responses after ALI (22). ALI leads to damage of alveolar epithelial cells due to a variety of direct and indirect causes (23). Evidence has suggested that miR-541-5p plays important roles in many organs (24–27). Studies have shown that miR-541-5p is a key effector in lung fibrosis and its
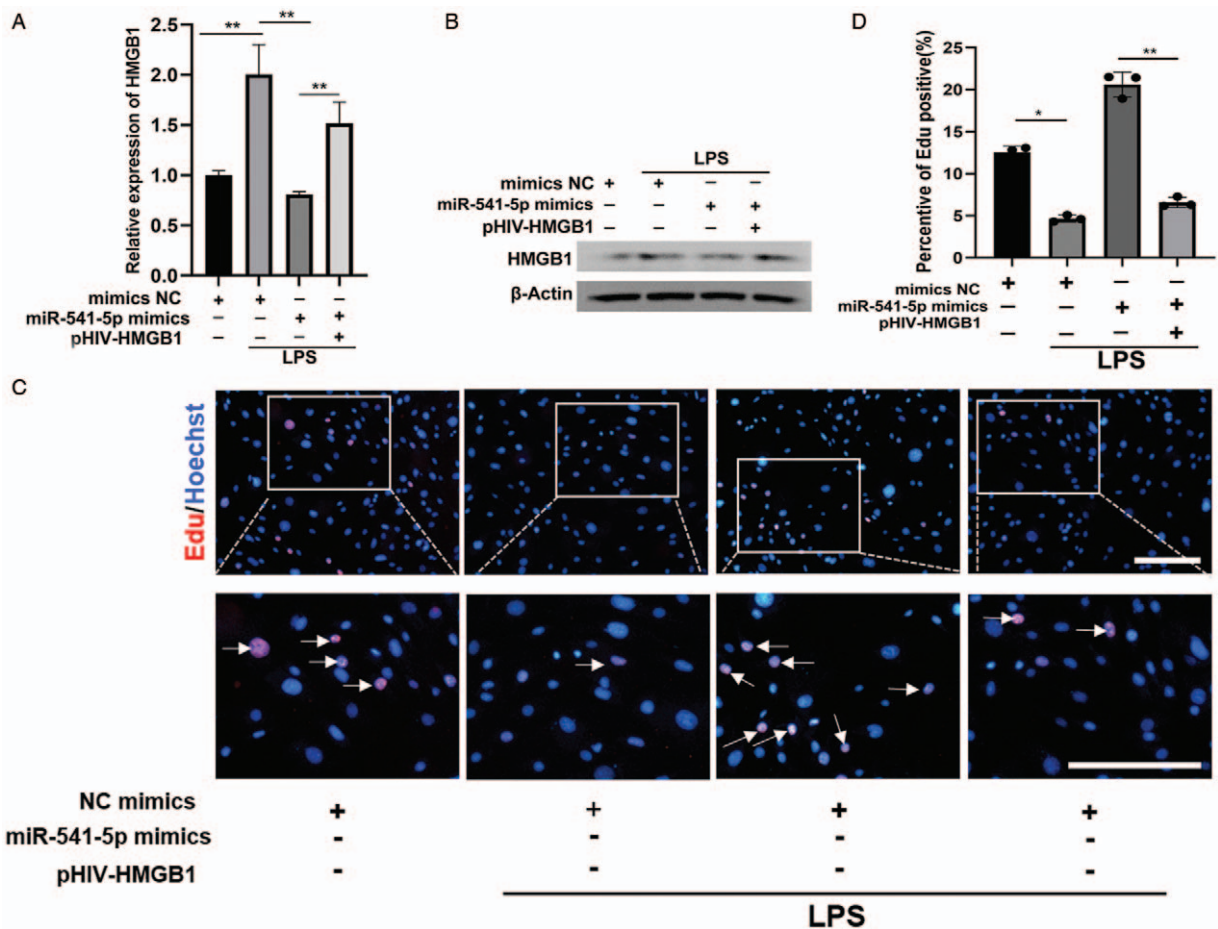

FIG. 5. **miR-541-5p/HMGB1 regulates ATII cell proliferation and activity via modulation of the JNK/ERK/p38pathway.** A, B, qPCR and western blot analyses of the expression of HMGB1 in ATII cells treated with NC mimics, LPS + NC mimics, LPS + miR-154-5p mimics, and LPS + pHIV-HMGB1. C, D, EdU assay analyses of the cell proliferation of ATII cells treated with NC mimics, LPS + NC mimics, LPS+miR-154-5p mimics, and LPS + pHIV-HMGB1. Data are presented as means ± SD of three individual experiments.β -Actin served as a control scare bar, 50 μm. *P < 0.05 and **P < 0.01.

overexpression is protective against lung fibrosis (24). However, the functional role of miRNAs in alveolar damage is largely unknown. In this study, we first demonstrated that miR-541-5p was decreased in ALI lung tissues and LPS-induced ATII cells, and that overexpression of miR-541-5p inhibited LPS-induced ATII cell proliferation and viability. Therefore, we speculate that miR-541-5p might be involved in the progression of ALI.

To investigate the involvement of cytokine and other mediators in ALI and LPS-induced ATII cells, we analyzed cytokine and chemokine expression levels by ELISA. There was higher expression of IL-6 and TNF-α in lung tissues after LPS intervention. Considering the role of HMGB1 in inflammatory progression, evidence suggests that HMGB1 plays a critical role in the pathogenesis of ALI. (28). In this study, we demonstrated that HMGB1 expression was dramatically increased in LPS-induced ALI tissues and LPS-induced ATII cells, and that inhibition of HMGB1 expression increased ATII cell proliferation and activation. In addition, dual luciferase reporter assay verified that miR-541-5p targeting HMGB1 in ATII cells directly regulates HMGB1 expression. Furthermore, we demonstrated that miR-541-5p suppressed the inflammatory response through HMGB1 activation.

As an essential signaling pathway protein, it has been demonstrated that the MAPK (mitogen-activated protein kinase) protein family is involved in ALI (29, 30). For instance, blocking of p-p38/p38, and the p-JNK/JNK signaling pathway alleviate the inflammatory response in ALI (29, 31). This finding demonstrates an association between ALI and MAPK. In our study, p-JNK, p-ERK, and p-p38, which belong to the MAPK family, were detected in LPS-induced ATII cells. We found that miR-541-5p is a key regulator of ATII cell proliferation and viability, and our results showed that miR-541-5p regulates cell proliferation and viability *in vitro*. Mechanistically, we found that HMGB1 binds to miR-541-5p, which thereby regulates the JNK/ERK/p38 pathway activity. This finding is significant as it suggests that modulation of the activity of miR-541-5p/HMGB1/JNK/ERK/p38 may be a potential therapeutic target for ALI.

Our study has some limitations. For instance, we only identified that miR-541-5p could restrain HMGB1 expression at the post-transcriptional level in ATII cells. Whether miR-541-5p could affect the expression of other key regulators of LPS-induced ATII cell proliferation and viability proliferation and viability needs further investigation.

CONCLUSIONS

In conclusion, our study provides new insights into the modulation of the biological progression of ATII cells. Our results illustrate that miR-541-5p/HMGB1 exerts an important role via modulation of the miR-541-5p/HMGB1 pathway in the LPS-induced ATII cell model. Overexpression of miR-541-5p attenuated LPS-induced ATII cell proliferation and viability *in vitro* via suppressing HMGB1 expression and upregulation of the JNK/ERK/p38 pathway, shedding light on the potential diagnosis and treatment of ALI in the future.

REFERENCES

1. Matthay MA, Zemans RL, Zimmerman GA, Arabi YM, Beitler JR, Mercat A, Herridge M, Randolph AG, Calfee CS: Acute respiratory distress syndrome. *Nat Rev Dis Primers* 5(1):18, 2019.
2. Li Z, Qin X, Bian W, Li Y, Shan B, Yao Z, Li S: Exosomal lncRNA ZFAS1 regulates esophageal squamous cell carcinoma cell proliferation, invasion, migration and apoptosis via microRNA-124/STAT3 axis. *J Exp Clin Cancer Res* 38(1):477, 2019.
3. Bellani G, Laffey JG, Pham T, Fan E, Brochard L, Esteban A, Gattinoni L, van Haren F, Larsson A, McAuley DF, et al.: Epidemiology, patterns of care, and mortality for patients with acute respiratory distress syndrome in intensive care units in 50 countries. *JAMA* 315(8):788–800, 2016.
4. Jansing NL, McClendon J, Henson PM, Tuder RM, Hyde DM, Zemans RL: Unbiased quantitation of alveolar Type II to alveolar Type I cell transdifferentiation during repair after lung injury in mice. *Am J Respir Cell Mol Biol* 57(5):519–526, 2017.
5. Hoffman AM, Ingenito EP: Alveolar epithelial stem and progenitor cells: emerging evidence for their role in lung regeneration. *Curr Med Chem* 19(35):6003–6008, 2012.
6. Song L, Zhou F, Cheng L, Hu M, He Y, Zhang B, Liao D, Xu Z: MicroRNA-34a suppresses autophagy in alveolar type ii epithelial cells in acute lung injury by inhibiting FoxO3 expression. *Inflammation* 40(3):927–936, 2017.
7. Fang Y, Gao F, Hao J, Liu Z: microRNA-1246 mediates lipopolysaccharide-induced pulmonary endothelial cell apoptosis and acute lung injury by targeting angiotensin-converting enzyme 2. *Am J Transl Res* 9(3):1287–1296, 2017.
8. Su ZQ, Mo ZZ, Liao JB, Feng XX, Liang YZ, Zhang X, Liu YH, Chen XY, Chen ZW, Su ZR, et al.: Usnic acid protects LPS-induced acute lung injury in mice through attenuating inflammatory responses and oxidative stress. *Int Immunopharmacol* 22(2):371–378, 2014.
9. Andersson U, Yang H, Harris H: High-mobility group box 1 protein (HMGB1) operates as an alarmin outside as well as inside cells. *Semin Immunol* 38: 40–48, 2018.
10. Kang R, Chen R, Zhang Q, Hou W, Wu S, Cao L, Huang J, Yu Y, Fan XG, Yan Z, et al.: HMGB1 in health and disease. *Mol Aspects Med* 40:1–116, 2014.
11. Song JH, Kim JY, Piao C, Lee S, Kim B, Song SJ, Choi JS, Lee M: Delivery of the high-mobility group box 1 box A peptide using heparin in the acute lung injury animal models. *J Control Release* 234:33–40, 2016.
12. Li R, Shang Y, Yu Y, Zhou T, Xiong W, Zou X: High-mobility group box 1 protein participates in acute lung injury by activating protein kinase R and inducing M1 polarization. *Life Sci* 246:117415, 2020.
13. Xiang M, Shi X, Li Y, Xu J, Yin L, Xiao G, Scott MJ, Billiar TR, Wilson MA, Fan J: Hemorrhagic shock activation of NLRP3 inflammasome in lung endothelial cells. *J Immunol* 187(9):4809–4817, 2011.
14. Corti M, Brody AR, Harrison JH: Isolation and primary culture of murine alveolar type II cells. *Am J Respir Cell Mol Biol* 14(4):309–315, 1996.
15. Xu L, Xue T, Zhang J, Qu J: Knockdown of versican V1 induces a severe inflammatory response in LPS-induced acute lung injury via the TLR2-NF-kappaB signaling pathway in C57BL/6J mice. *Mol Med Rep* 13(6):5005–5012, 2016.
16. Janga H, Cassidy L, Wang F, Spengler D, Oestern-Fitschen S, Krause MF, Seekamp A, Tholey A, Fuchs S: Site-specific and endothelial-mediated dysfunction of the alveolar-capillary barrier in response to lipopolysaccharides. *J Cell Mol Med* 22(2):982–998, 2018.
17. Barkauskas CE, Cronce MJ, Rackley CR, Bowie EJ, Keene DR, Stripp BR, Randell SH, Noble PW, Hogan BL: Type 2 alveolar cells are stem cells in adult lung. *J Clin Invest* 123(7):3025–3036, 2013.
18. Fehrenbach H: Alveolar epithelial type II cell: defender of the alveolus revisited. *Respir Res* 2(1):33–46, 2001.
19. Zheng S, Yang J, Hu X, Li M, Wang Q, Dancer RCA, Parekh D, Gao-Smith F, Thickett DR, Jin S: Vitamin D attenuates lung injury via stimulating epithelial repair, reducing epithelial cell apoptosis and inhibits TGF-beta induced epithelial to mesenchymal transition. *Biochem Pharmacol* 177:113955, 2020.
20. Li W, Qiu X, Jiang H, Han Y, Wei D, Liu J: Downregulation of miR-181a protects mice from LPS-induced acute lung injury by targeting Bcl-2. *Biomed Pharmacother* 84:1375–1382, 2016.
21. Ke XF, Fang J, Wu XN, Yu CH: MicroRNA-203 accelerates apoptosis in LPS-stimulated alveolar epithelial cells by targeting PIK3CA. *Biochem Biophys Res Commun* 450(4):1297–1303, 2014.

22. Vaporidi K, Vergadi E, Kaniaris E, Hatziapostolou M, Lagoudaki E, Georgopoulos D, Zapol WM, Bloch KD, Iliopoulos D: Pulmonary microRNA profiling in a mouse model of ventilator-induced lung injury. *Am J Physiol Lung Cell Mol Physiol* 303(3):L199–207, 2012.

23. Barr LC, Brittan M, Morris AC, McAuley DF, McCormack C, Fletcher AM, Richardson H, Connell M, Patel D, Wallace WA, et al.: A randomized controlled trial of peripheral blood mononuclear cell depletion in experimental human lung inflammation. *Am J Respir Crit Care Med* 188(4):449–455, 2013.

24. Raghunath A, Jeyabaskar D, Sundarraj K, Panneerselvam L, Perumal E: In silico prediction of microRNAs on fluoride induced sperm toxicity in mice. *Food Chem Toxicol* 98(pt A):34–49, 2016.

25. Ren L, Yang C, Dou Y, Zhan R, Sun Y, Yu Y: MiR-541-5p regulates lung fibrosis by targeting cyclic nucleotide phosphodiesterase 1A. *Exp Lung Res* 43(6–7):249–258, 2017.

26. Moradi S, Sharifi-Zarchi A, Ahmadi A, Mollamohammadi S, Stubenvoll A, Gunther S, Salekdeh GH, Asgari S, Braun T, Baharvand H: Small RNA sequencing reveals Dlk1-Dio3 locus-embedded MicroRNAs as major drivers of ground-state pluripotency. *Stem Cell Reports* 9(6):2081–2096, 2017.

27. Qi Y, Wang D, Huang W, Wang B, Huang D, Xiong F, Chen X, Chen Y: CyclinD1 inhibits dicer and crucial miRNA expression by chromatin modification to promote the progression of intrahepatic cholangiocarcinoma. *J Exp Clin Cancer Res* 38(1):413, 2019.

28. Meng L, Li L, Lu S, Li K, Su Z, Wang Y, Fan X, Li X, Zhao G: The protective effect of dexmedetomidine on LPS-induced acute lung injury through the HMGB1-mediated TLR4/NF-kappaB and PI3K/Akt/mTOR pathways. *Mol Immunol* 94:7–17, 2018.

29. Li D, Ren W, Jiang Z, Zhu L: Regulation of the NLRP3 inflammasome and macrophage pyroptosis by the p38 MAPK signaling pathway in a mouse model of acute lung injury. *Mol Med Rep* 18(5):4399–4409, 2018.

30. Chen LJ, Ding YB, Ma PL, Jiang SH, Li KZ, Li AZ, Li MC, Shi CX, Du J, Zhou HD: The protective effect of lidocaine on lipopolysaccharide-induced acute lung injury in rats through NF-kappaB and p38 MAPK signaling pathway and excessive inflammatory responses. *Eur Rev Med Pharmacol Sci* 22(7):2099–2108, 2018.

31. Jin B, Jin H: Oxymatrine attenuates lipopolysaccharide-induced acute lung injury by activating the epithelial sodium channel and suppressing the JNK signaling pathway. *Exp Anim* 67(3):337–347, 2018.